Evaluation of devolatilization behaviour of different carbonaceous materials under rapid heating for the novel HIsarna ironmaking process

Darbaz Khasraw [a,*], Stephen Spooner [a], Hans Hage [b], Koen Meijer [b], Zushu Li [a]

[a] WMG, University of Warwick, Coventry, UK

[b] Tata Steel, IJmuiden 1970 CA, The Netherlands

HIGHLIGHTS

- **Rapid devolatilization of different carbononaceous materials investigated for the HIsarna alternative ironmaking process**
- **Rapid heating via drop tube furnace with quadrupole mass spectrometer (DTF-QMS)**
- **Explained the effect of temperature on variation of light gases in the rapid devolatilization**
- **Revealed the effect of temperature on the rate of carbon conversion for coal and charcoal.**
- **R-factor parameter obtained to give an indication of how efficiently the carbon material can yield solid char residuals under the HIsarna atmosphere.**

Abstract: A drop-tube furnace coupled with quadrupole mass spectrometer (DTF-QMS) was employed to simulate rapid heating conditions that carbonaceous materials experience during HIsarna injection with the measurement of gas composition change as a result. A devolatilization study for thermal coal (TC) and charcoal (CC) samples was carried out at three temperatures of 1000, 1250 and 1500 °C under an initial high purity Ar gas environment. The volatiles released were measured online by QMS, while the char yield was determined directly by the weight of particles collected and the deficit was calculated by subtracting the gas yielded from the total

weight loss. The study reveals that working temperature has a strong impact on the devolatilization rate, the maximum weight loss and the variation in gas species produced. Due to intensification in the carbon oxidation and secondary reactions at higher temperatures, there was an increase in the weight loss, which led to a greater yield of H_2 and CO but less yield of hydrocarbons, CO_2 and H_2O. Despite lower volatile matter content in charcoal, the weight loss for charcoal (29%) was higher than that for thermal coal (23%) at 1500 °C. Although the amount of H_2 produced for both materials is similar, the amount of CO produced by charcoal is twice of that by thermal coal, and accounts for 79% of the total gas weight formed by charcoal. This suggests that a higher rate of carbon oxidation takes place through O_2 containing groups within the charcoal, which results in lower char efficiency. It was found that thermal coal produces a significant amount of tar, while a large number of particles in the form of soot/dust escaped from the bulk material during charcoal injection but no tar formation was observed.

Keywords:

HIsarna technology

Coal and charcoal

Rapid devolatilization

Devolatilization products

Drop tube furnace (DTF)

Quadrupole mass spectrometer (QMS)

* **Corresponding author. Tel.: +44 (0)24 7652 4706;**

E-mail address: d.khasraw@warwick.ac.uk (D. Khasraw)

Postal address: WMG, University of Warwick, Coventry CV4 7AL, UK

1. Introduction

Steel manufacturing consumes a large quantity of carbon, which makes the steel industry one of the biggest carbon dioxide (CO_2) emitters worldwide as an industry (with only cement/concrete industries producing more). The ironmaking process including sintering, coke making and blast furnace (BF) accounts for approximately 90% of CO_2 output from an integrated BF-BOF (basic oxygen steelmaking) steel plant [1], [2]. The increase in demand for steel and stricter environmental legislation due to concerns about global warming and climate change have forced steel manufacturers to undertake extensive research and development to reduce CO_2 emissions without compromising the process efficiency or increasing product costs significantly [3].

The HIsarna process is a novel ironmaking technology developed under the European Ultra-Low CO_2 steelmaking (ULCOS) program, with the aim of reducing CO_2 emissions by at least 50% compared to the blast furnace ironmaking route [4]. HIsarna is a smelting reduction process, which combines the Cyclone Converter Furnace (CCF) and the Smelting Reduction Vessel (SRV) to a single smelting furnace as shown in Figure 1. The HIsarna pilot plant located in Tata Steel IJmuiden, the Netherlands was constructed in 2010 with a capacity of 8 ton/hr [5], [6]. The process flexibility with regards to raw materials results in the removal of a number of pre-processing steps (e.g. sintering and coke making), which alone reduces CO_2 emission by 20 % and when all benefits of the process are considered there is a potential for more than 80 % CO_2 reduction with the addition of carbon capture, usage and storage (CCUS) [4], [6]. As a smelting

technology, HIsarna offers the ability to completely substitute the current coking coal usage with renewable biomass, while maintaining process efficiency and productivity [7].

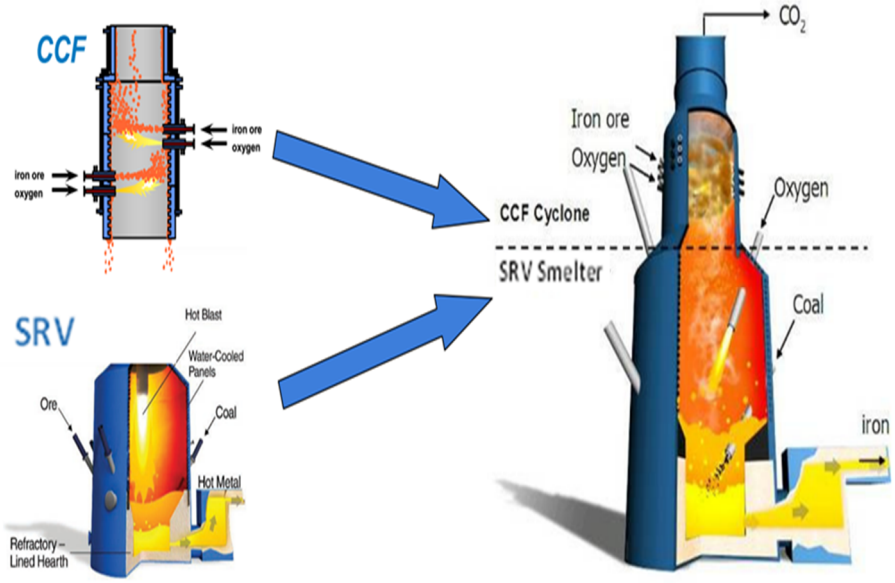

Figure 1. A schematic of HIsarna technology combining the CCF and SRV [8].

The HIsarna process begins with an injection of fine iron ore particles together with high purity oxygen into the CCF, where the CO rich hot gas evolved from SRV is combusted to increase the temperature to approximately 1450 °C and cause the iron ore to melt. Also in the cyclone a pre-reduction rate of up to 20% is achieved through thermal decomposition of ores and reduction by the post-combustion gases arising from the SRV [9], [10]. The molten and partially reduced ore will flow down the wall of the cyclone and drip into the slag layer of the SRV, where granular coal (or other carbonaceous materials) is injected to fully reduce the iron ore through a route of dissolution and subsequent metal slag reactions [6].

Once the solid carbonaceous material is injected into the SRV, the particles rapidly go through a series of physical and chemical changes due to the extreme high temperatures (up to 1500 °C). Devolatilization is the first step, which results in the release of volatile matter (condensable and

light gases), while the solid structure goes through dramatic transformation due to phenomena such as softening, swelling and fragmentation [11], [12], [13]. The volatile matter released and the CO produced from carbon-slag reaction will increase a hot gas stream upward to enable partial reduction of ore and maintain the temperature in the CCF because of post-combustion. The remaining chars will dissolve into the hot metal and react with iron oxide in the slag in the SRV. The main gas species evolved during devolatilization step are H_2, CO, CO_2, H_2O and light hydrocarbons including CH_4 and C_2H_6, the balance of which will change the reducing environment and control the temperature throughout the full HIsarna technology [14]. Pre-reduction of iron ore in the cyclone is an essential step which needs to be studied to optimise HIsarna's operation and achieve high efficiency. Therefore, the reduction kinetics, melting and pre-reduction behaviour of hematite ore has been studied in reaction conditions of the smelting cyclone. To achieve these studies, thermal decomposition of hematite ore, and variation of temperature, particle size and gas concentration have been considered [9], [10], [15]–[18], while for gas composition variation effects on the reduction degree, the gas mixture with different post combustion ratios (PCR) was characterized at the temperature of 1377 °C [18]. It was found that thermal decomposition degree of hematite increases with the increase of temperature [16], while reduction degree decreases with the increase of post combustion ratio (PCR) and particle size [16], [18]. The PCR is defined as equation (1) [17]:

$$PCR = \frac{\%CO_2+\%H_2O}{\%CO_2+\%CO+\%H_2O+\%H_2} X\ 100 \quad (1)$$

The devolatilization of carbonaceous materials injected into SRV provides gases for indirect reduction (e.g. reduction of iron ore by CO) and heat balance via post combustion in both SRV and CCF. Thus this is integral to understanding the balance of productivity and heat during the pre-reduction of iron ore in CCF, which is considered as the first step of the process. In order to select the right mix of carbonaceous materials such as replacing thermal coal with biomass, it is

106 essential to evaluate the devolatilization behaviour of different carbonaceous materials under
107 HIsarna's thermal conditions (e.g. rapid heating and high temperature). Various factors may
108 impact the devolatilization of the carbonaceous materials, such as structure, chemical
109 composition and particle size of the carbonaceous materials, temperature, pressure, heating
110 rate and reaction atmosphere [19]. A large number of studies have been performed to
111 investigate gaseous product evolution at relatively low temperatures around 1000 °C and low
112 heating rates of <1 °C/s using TGA-MS technique [19]–[24]. However, when carbon particles are
113 injected into SRV where the temperature is up to 1500 °C, it can experience an extremely high
114 heating rate of 10^4-10^5 °C/s [11][25].

115 Several techniques have been used to study the effect of rapid heating on carbonaceous
116 materials devolatilization [12]–[14], [25]–[35]. Most of these experiments have been conducted
117 at a relatively low final temperature up to 1000 °C, focusing on the characterization of char
118 generated under high heating rates. For example, a wire mesh reactor (WMR) was used to study
119 gas evolution from coal primary pyrolysis at heating rates of 500-1000 °C/s, and using gas
120 chromatography and an FTIR spectrophotometer for gas analysis. It was found that the gaseous
121 product yield increased with increasing pyrolysis temperature up to 1100 °C [14], [30]. The
122 isothermal plug flow reactor (IPFR) was used to study the effect of rapid heating on biomass
123 material with three torrefaction degrees, the reactivity of the chars was determined by
124 calculating weight loss through the ash tracer method and it was found that the biomass with
125 higher torrefaction has lower reactivity [32]. The filament platinum pyrolyzer [31], custom made
126 thermogravimetric analysis (TGA) furnace [33] and the drop tube furnace method [13], [26]–
127 [29], [34], [35] have all been used to produce chars through rapid heating to different final
128 temperatures. The solid char particles produced via these experimental techniques were used
129 for further analysis to investigate the effect of different rapid heating conditions on char

130 formation. By performing TGA, SEM and the ash tracer method on the remaining chars, the
131 kinetic parameters, morphology and the char reactivity were determined to help predict char
132 gasification behaviour in the gasification plants. Through these investigations it was observed
133 that higher pyrolysis temperatures produce more reactive chars, due to the formation of pores
134 and roughness on the char surface. Yan et al [12] studeid the effects of coal properties, particle
135 ultimate temperature and heating rate on coal devolatilization perfromances using a drop tube
136 furance and a lab-scale plasma reactor. This study revealed that fast pyrolysis of coal would
137 greatly increase the yield of light gases compared to a slow pyrolysis process. Zhang et al [31]
138 investigated higher temperature (1000~1300 °C) pyrolysis behaviour in a drop tube furnace with
139 focus on the physiochemical characeristics and reation kinetics of the resultant char, it was
140 found that higher temperature results in more CO but less CH_4. The study also reveals that
141 temperature incease develops more pore structures and due to upgrade in the coal rank the
142 activation energy increases for combution of resultant chars.

143 The devolatilization behaviour of thermal coal and biomass under HIsarna's thermal conditions
144 (fast heating to high temperature up to 1500 °C) is an area which requires further investigation
145 in order to understand the potential of the HIsarna process compared to the typical conditions
146 covered in the literature. In order to select the right mixture of carbonaceous materials (e.g.
147 substitution of coal with certain biomasses), and to ensure proper reduction (indirect reduction
148 in SRV and pre-reduction in CCF) and heat balance (via post combustion), it is necessary to obtain
149 accurate information of volatile matter yields, gaseous products, and their releasing rates under
150 the thermal conditions similar to the HIsarna process. In this study, a drop tube furnace coupled
151 with an online quadrupole mass spectrometer (DTF-QMS) was employed to evaluate the
152 devolatilization behavior of thermal coal and biomass under thermal conditions similar to

HIsarna (rapid heating to high temperature up to 1500 °C), focusing on volatile matter yields, gaseous products and their evolving rates.

2. Materials and methods

2.1. Sample preparation

Two different carbon sources, a thermal coal (TC) with a medium volatile matter content and a charcoal (CC) (a Birch wood based pre-treated biomass), were used in this work to study devolatilization behaviour under rapid heating. Both materials are provided by Tata steel IJmuiden, and have already been used for HIsarna injection during the pilot plant trials. The samples were dried at 80 °C for 12 hours to ensure the removal of all the surface moisture, and then crushed into small particles with the size range from 90 to 300 µm to be tested. Table 1 shows the proximate and ultimate analysis data for the two samples.

Table 1. Proximate and ultimate values of the used thermal coal (TC) and charcoal (CC)

	TC	CC
Moisture/ % (ad)	8.87	4.56
Proximate Analysis wt% (db)		
Volatile Matter	22.18	12.1
Ash	8.8	1.8
Fixed Carbon (by difference)	69.02	86.1
Ultimate Analysis wt% (db)		

Carbon	81.91	89.4
Hydrogen	4.27	3.11
Nitrogen	2.19	0.57
Sulphur	0.24	0.06
Oxygen by (difference)	2.59	5.06

db – dry basis; ad – air dried

2.2. Experimental method

2.2.1. Devolatilization

The devolatilization experiments were performed using a Carbolite-Gero high temperature vertical tube furnace with a recrystallized alumina tube (VTF-1700/50, internal diameter 88 mm x length 1000 mm) schematically shown in Figure 2. The furnace was coupled with a Hiden HPR 20 Quadrupole Mass Spectrometer (QMS) to monitor gaseous products evolving from the samples during devolatilization. To protect the QMS from soot and condensable tar, disposable inline filter (Parker 1/4in G nylon) with maximum flow rate and working temperature of 152 L/min and 110 °C respectively was installed along the connection line. The combination of DTF-QMS allowed the carbonaceous material samples to be rapidly heated to pre-set temperatures of 1000, 1250 and 1500 °C at the heating rate of approximately 10^4–10^5 °C/s [25], while the off-gas was continuously analysed. The carbon particles were injected into the pre-set temperature region through a particle feeder designed using a tee piece connected two ball valves and an argon line to create an inert atmosphere and carry the particles shown in Figure 2. The particle feeder was mounted to the top water cooled flange and directly connected to an alumina lance (internal diameter 5 mm) which was inserted through the flange into the reactors hot zone.

Before the experiment starts a sample of approximately 100 mg was placed on the seat of the bottom ball valve while in the “off” position, and an Ar (with a 99.999% purity) flush through the feeder was conducted to create an oxygen-free atmosphere before all valves were closed. While the furnace heated to the desired temperature at a heating rate of 10 °C/min, a carrier gas (Ar, 99.999% purity) at 1 L/min was purged through the furnace from the bottom to ensure an inert atmosphere.

When the furnace temperature reached the experimental temperature, the valve holding the sample was opened, at the same time the valve controlling the Ar gas was switched to the feeder for ~10 seconds to maintain the atmosphere, while the samples were injected. The Ar gas also carried the sample particles to the crucible placed in the centre of the isothermal region in the furnace. The whole sample was fed at once to ensure it reach the desired place and temperature at the same time. The furnace was kept at the pre-set temperature for a total of 10 minutes while the furnace exhaust was connected to the QMS through a heated capillary (150 ^{o}C) to monitor gaseous products evolving from the samples while ensuring no condensation occurred before the ionization chamber. The QMS was set to measure readings of the following gaseous products: N_2, O_2, CO, CO_2, Ar, H_2O, H_2, CH_4 and C_2H_6. After the reaction time was completed the furnace was cooled down at the rate of 5 °C/minutes to room temperature in an Ar atmosphere and the char particles were collected in the alumina crucible for further analysis.

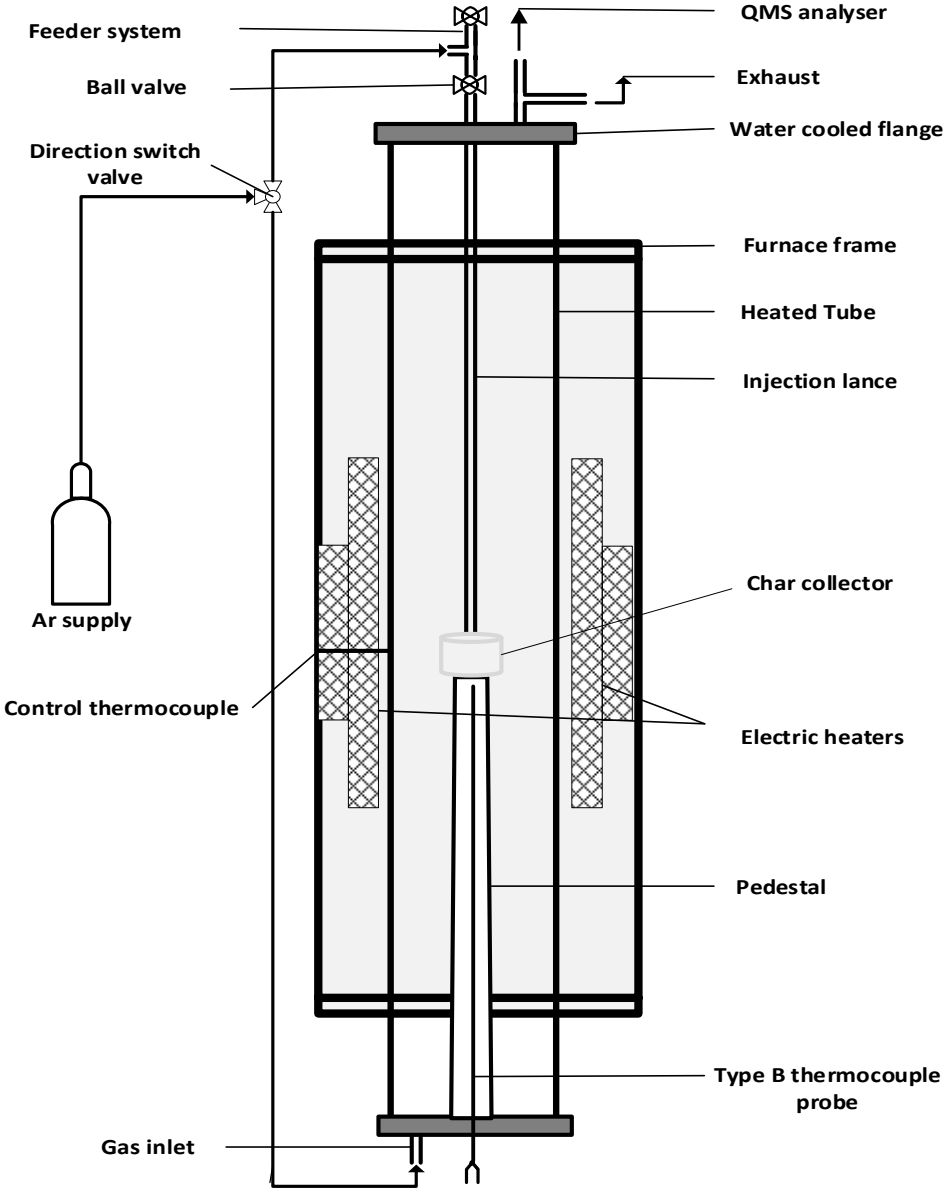

200

201 *Figure 2. Drop tube furnace (DTF) setup with a mass spectrometry for rapid devolatilization study.*

202 *The quadrupole mass spectrometer QMS is connected to the gas sampling port.*

203 **2.2.2. Char yield**

204 The char yield was directly determined during devolatilization of the carbonaceous materials in

205 the DTF at the temperatures of 1000, 1250 and 1500 °C. The material fed into the DTF was

206 weighed before and after the heat treatment to calculate the weight loss. To validate the

method and confirm good collection efficiency a series of experiments were perform in the DTF (as shown in Figure 2), at ambient temperature for each carbonaceous material. Three trails were performed using the same particle size used during the devolatilization experiments. Figure 3 shows the amount of materials collected in the alumina crucible placed in the centre of the hot-zone during validation trials. The weight of collected material was very close to the weight of fed material with an average of 99.1% and 96.13% of the fed materials collected for TC and CC respectively. CC was found to be less efficient with this configuration which could be due to the physical properties of CC such as low density and less spherical particle shapes. Therefore during the devolatilization experiments the sample weights were adjusted according to the expected mass balance shown in Figure 3 to ensure the correct calibrated mass of each sample was recorded after devolatilization tests. Devolatilization experiments were repeated three times at each temperature to produce concordant results.

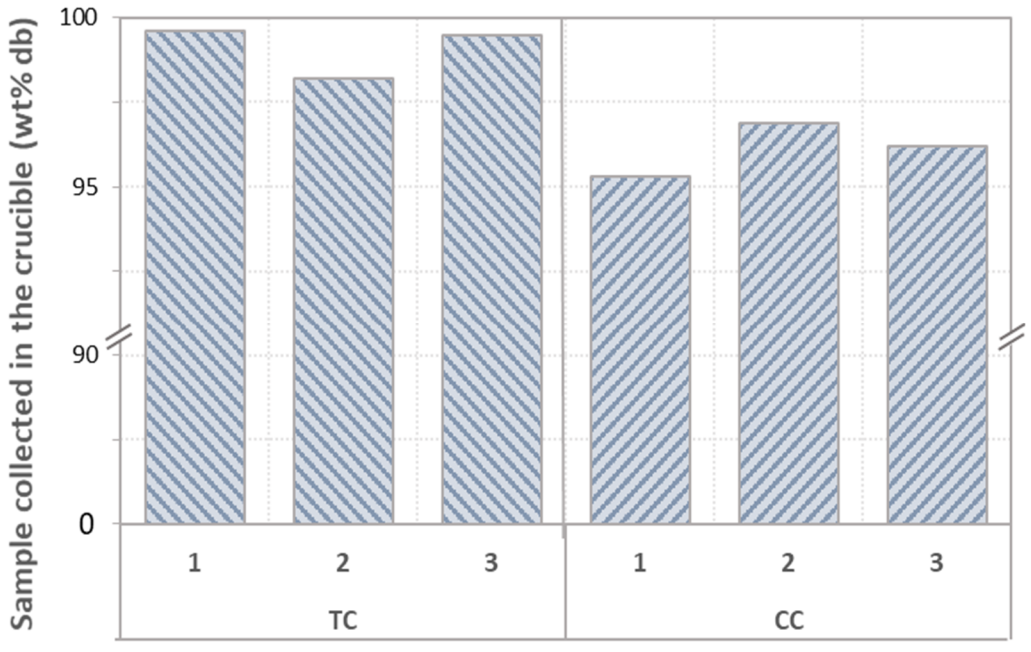

Figure 3. The amounts of carbon material particles collected in the crucible placed in the centre of DTF, after fed into the reactor at ambient temperature passing through the injection lance.

2.2.3. R-factor determination

The R-factor is an important parameter which is normally used to evaluate the feasibility of coal use for injection in the blast furnace process [35]. The R-factor stands for the volatile release ratio, which compares the weight loss that occurs under rapid heating conditions of carbon materials to the standardised volatile matter (VM) content. A high R-factor value means high carbon conversion to volatiles and less solid char residuals. The equation below shows how the R-factor is calculated assuming the ash of the carbon material is inert:

$$R - factor = \frac{V}{Prox\ VM\ content\ (dry\ ash\ free)} \quad (2)$$

where *V* represents the total volatile yield, measured by difference in weight of the starting and collected material.

2.2.4. Raman Spectroscopy

Raman spectroscopy is one of the most common techniques used to study characteristics of carbonaceous materials [36]–[39]. The Raman spectra of the TC and CC chars produced during injection at 1500 °C were obtained with an excitation laser at 514.4 nm and grating of 1800 l/mm using Renishaw InVia Reflex Raman Spectrometer. Particles of each char samples were placed on a slide and were focused using a 20X objective lens. The Raman Spectra in the region 100 – 3500 cm^{-1} were collected, however the spectra range between 800 - 1900 cm^{-1} produces the most pertinent information on the degree of structural disorder of carbonaceous materials [37]. In order to study the degree of graphitic structure and evaluate its effect on the devolatilization behaviour of different carbon sources under HIsarna thermal conditions, the Raman spectra obtained in the range of 800 - 2000 cm^{-1} for TC and CC chars were analysed and presented in Figure 4.

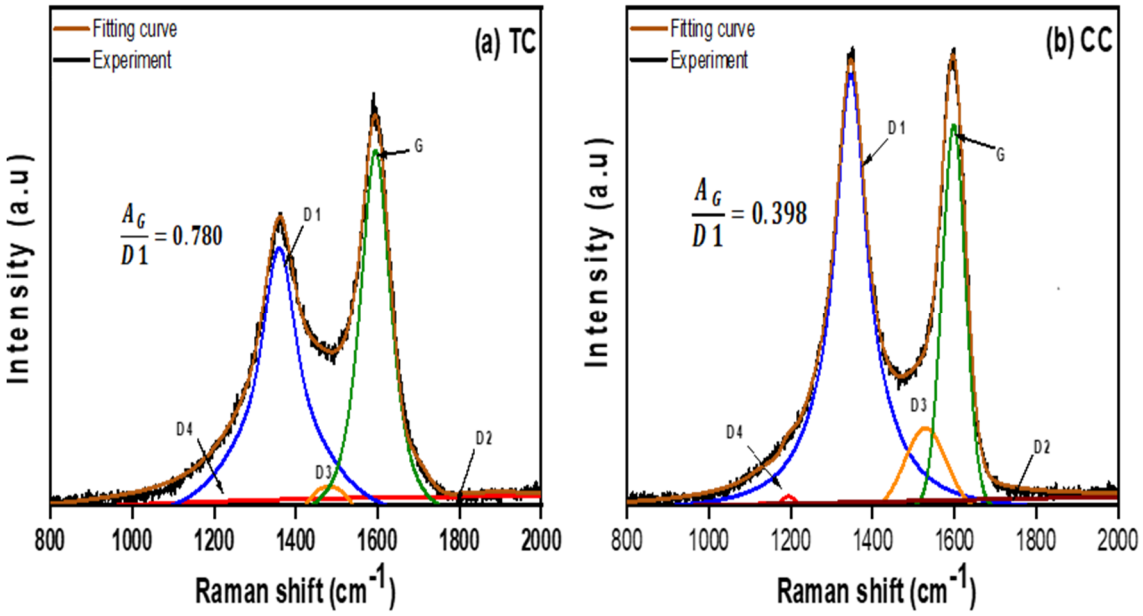

244

245 *Figure 4. Raman spectra and peak fitting of (a) thermal coal char and (b) charcoal char produced*
246 *during 1500 °C injection.*

247 For this Raman spectra range carbonaceous materials can produce up to five characteristic
248 spectra bands, which can be resolved into five peaks (D1, D2, D3, D4 and G) [40]. However, the
249 spectra in Figure 4 show that only two significant peaks appeared at a shift of ~1350 cm^{-1} and
250 ~1600 cm^{-1}, corresponding to the D and G bands. It is well known that the spectra band
251 positioned at 1360 cm^{-1} reveals weakness and disorder in the carbon structure while the spectra
252 band at 1600 cm^{-1} represents the vibration of the ideal graphite lattice [37]. To determine the
253 precise detailed differences of spectral features between TC and CC, relevant spectra bands
254 were fitted to pseudo-Voigt function using originPro 2019b to calculate area, bandwidth and
255 relative intensities. The ratio of the intensity of G/D1 is known to determine the order degree of
256 carbon structure with greater ratio indicating more ordered graphite structure in the
257 carbonaceous material. To obtain more accurate results, the area ratio ($\frac{A_G}{A_{D1}}$) for TC and CC
258 calculated is approximately 0.780 and 0.398 respectively. The area ratio for CC char is much
259 lower than that for TC char, which confirms charcoal has less ordered graphite structure and it

is more amorphous carbon implying its being more reactive [41]. Therefore, it can be speculated that more disordered structure for CC will enhance its devolatilization rate.

3. Results and discussion

3.1. Effect of temperature on devolatilization behaviour

In order to compare the effect of temperature on devolatilization behaviour, the DTF experiments for TC and CC were conducted at three different temperatures of 1000, 1250 and 1500 °C. Typical variations in the measured rate of volatile matter release with the change in temperature are given in Figure 5. An instant devolatilization reaction was observed from the gas formation curves at all three temperatures, however there was a few seconds delay in the detection of the gases by the online QMS due to the travelling distance in the DTF tube. This conversely led to the continued detection of devolitization gases for a period of time after the process was completed as these gases passed through the remainder of the furnace.

The QMS was set to analyse CO, CO_2, H_2O, H_2, CH_4 and C_2H_6 gases, which are the main gas species produced during thermal treatment of carbon materials (determined through a calibration run where m/z (the mass-to-charge ratio) 0-50 was scanned throughout a devolitization test to detect all species emitted). The formation of CO_2 and CO in the carbon materials is linked to decomposition of oxygen containing functional groups, but H_2 and hydrocarbons are formed from decomposition of heterocyclic and methyl groups. H_2O release is linked to the decomposition of different oxygen containing groups mainly OH groups [14, 24, [23].

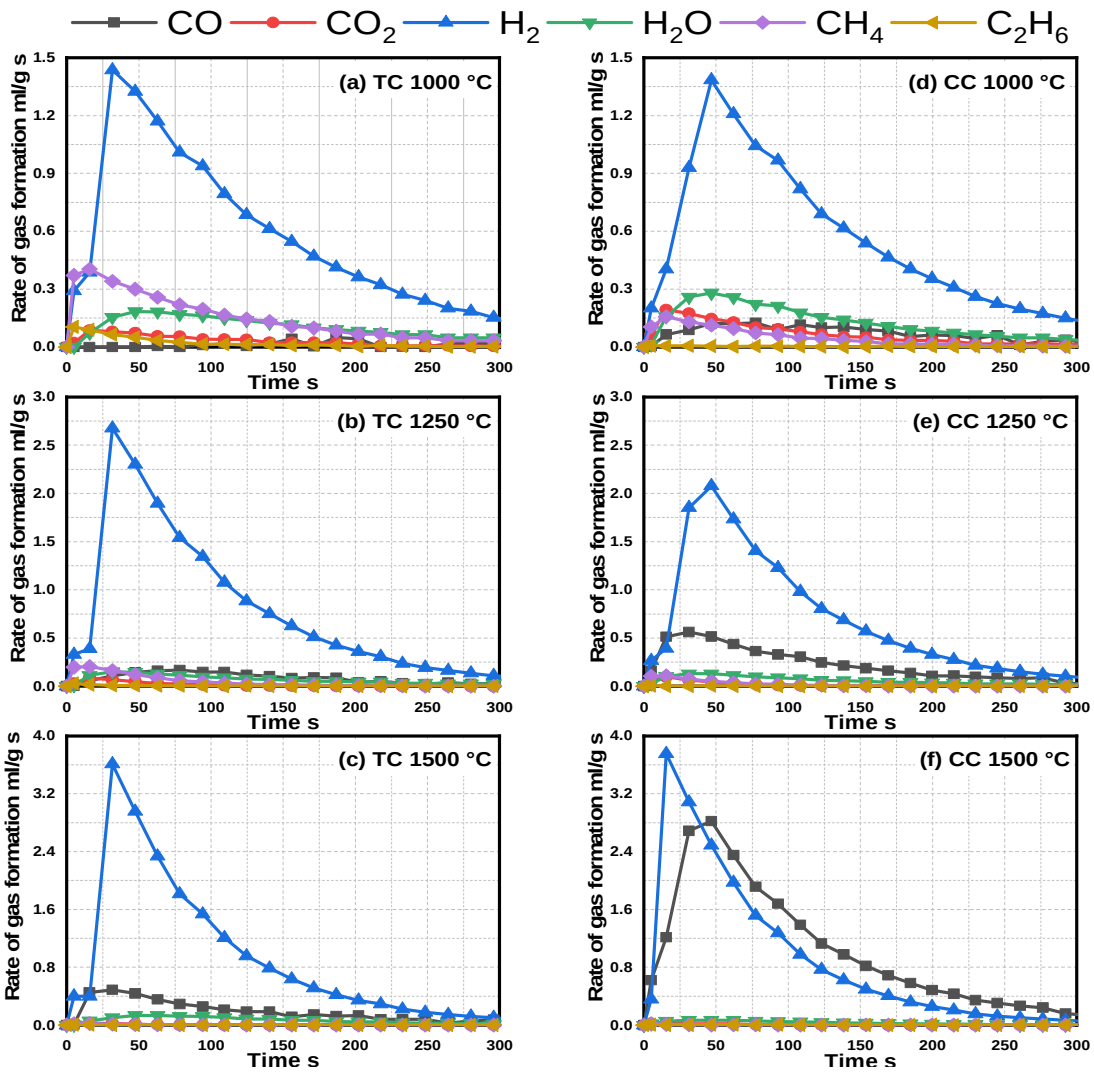

Figure 5. Rate of formation of gas species (CO, CO_2, H_2, H_2O, CH_4, and C_2H_6) for thermal coal (a, b and c) and charcoal (d, e and f) at temperatures of 1000, 1250 and 1500 °C respectively in a high purity argon atmosphere.

Some common phenomena can be observed for both samples as can be seen in Figure 5. The gas variation behaviour between the two samples is similar at three temperatures measured, and the evolution rate of H_2 is shown to be the highest out of all gas species. At 1000 °C, compared with CC, the rate of evolution of H_2 and hydrocarbon for TC was higher and the devolatilization time was slightly longer. A lower evolution rate and shorter devolatilization time

288 for charcoal could be related to the fact that CC has already been pre-treated to several hundred
289 degrees during production and as such lower molecular weight/lower boiling point volatiles may
290 have already undergone some devolatilization. However, higher O_2 content in CC caused the
291 material to produce much more CO, CO_2 and H_2O in comparison to thermal coal. As shown in
292 Figure 5, the rate of gas formation for CO_2, H_2O, CH_4 and C_2H_6 reached maximum values for both
293 samples at the temperature of 1000 °C. By increasing temperature, the carbon conversion for
294 both materials increased significantly. It is also observed that the formation rate of both CO and
295 H_2 increased, while CO_2, H_2O, CH_4 and C_2H_6 contents decreased sharply.

296 Figure 6 shows the yield variations for all major gaseous species produced under rapid
297 devolatilization conditions for CC. As shown in Figure 6(b), the yield of CO_2 decreased with
298 increasing temperature from 1000 to 1500 °C. At 1250 °C the yield of CO_2 decreases rapidly to
299 the lowest value by the time of ~100 seconds. The yield of CO_2 reduced further with increasing
300 the temperature to 1500 °C but a small amount of CO_2 was still detected, which may have
301 evolved and escaped before any secondary reactions had taken place. Similar behaviour was
302 observed for H_2O (Figure 6(d)), its yield decreased with increasing temperature from 1000 to
303 1500 °C and a small amount of H_2O was still detected at 1500 °C. The evolution of CH_4 (Figure
304 6(e)) followed the similar trend, its yield decreased with increasing temperatures, however, CH_4
305 was almost completely converted at 1500 °C by 50 seconds.

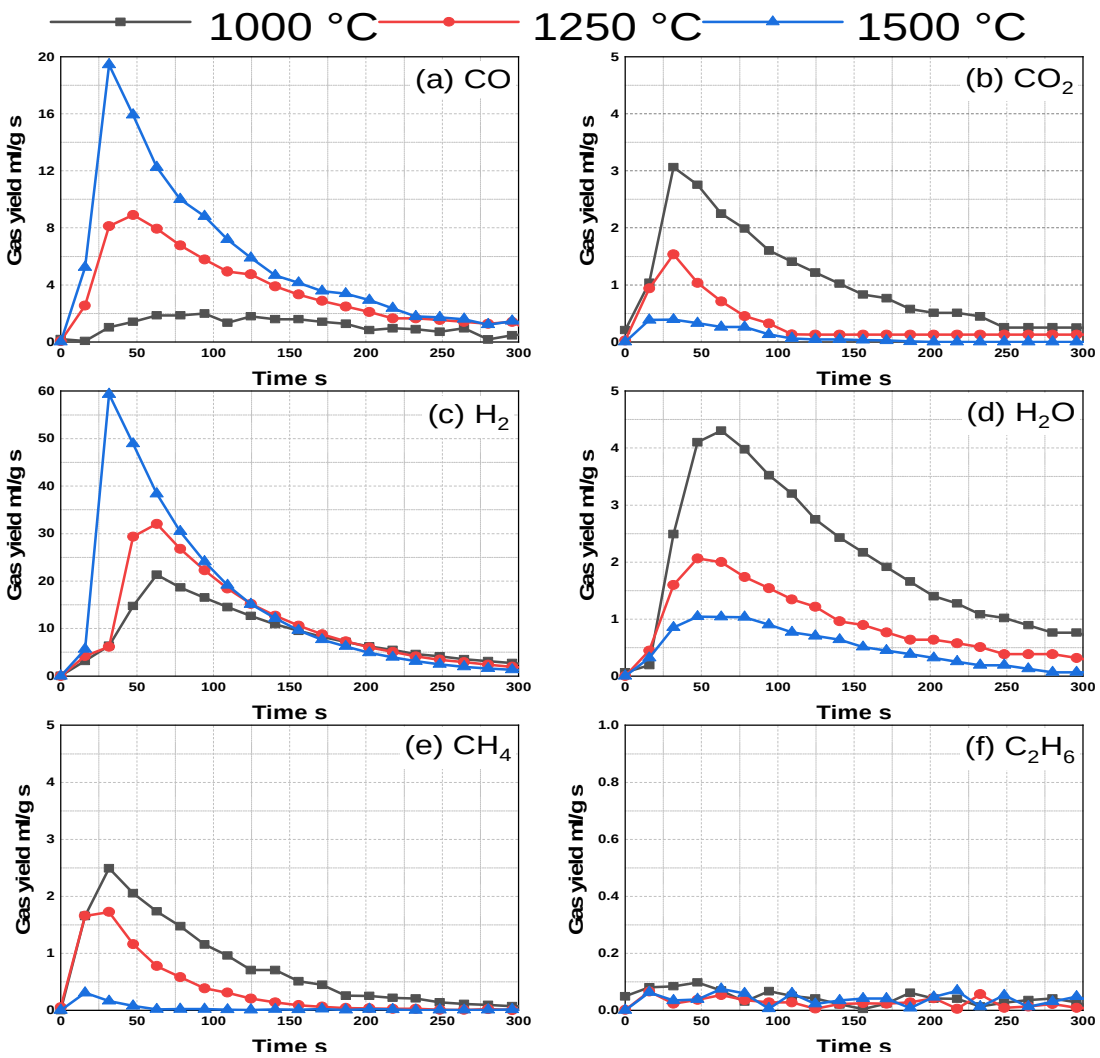

Figure 6. An off-gas analysis of (a) CO; (b) CO_2; (c) H_2; (d) H_2O; (e) CH_4; and (f) C_2H_6 produced during rapid devolatilization experiments for CC under argon atmosphere at three ultimate temperatures of 1000, 1250 and 1500 °C.

As shown in Figure 6 both H_2 and CO yield increase quite significantly with an increase in the temperature and they are the main components of released volatiles at a temperature of 1500 °C. Although some of the CO and H_2 are generated at high temperature from decomposition of oxygen and hydrogen containing compounds, it is believed that carbon oxidation reactions through CO_2 and H_2O and other secondary reactions are taking place which results in an increase in these gas components [25]. In addition, the temperature increase results in the secondary tar

316 cracking reactions which can partially convert tar into light hydrocarbons and contributes to an
317 increase in the yield of CO [12]. The light hydrocarbons evolved at higher temperatures will react
318 with CO_2 and H_2O to form H_2 and CO [24], [42], [43]. The carbon oxidation and the secondary
319 reactions are shown in equations (3) to (6):

320 $$C_{(S)} + CO_{2\,(g)} \rightarrow 2CO_{(g)} \quad (3)$$

321 $$C_{(s)} + H_2O_{(g)} \rightarrow CO_{(g)} + H_{2\,(g)} \quad (4)$$

322 $$CO_{2\,(g)} + CH_{4\,(g)} \rightarrow 2CO_{(g)} + 2H_{2\,(g)} \quad (5)$$

323 $$H_2O_{(g)} + CH_{4\,(g)} \rightarrow CO_{(g)} + 3H_{2\,(g)} \quad (6)$$

324 Furthermore, the thermal cracking of hydrocarbons is possible at temperature > 600 °C, cracking
325 reactions can take place rapidly with an increase in temperature and decompose to H_2 and soot
326 (solid carbon dust with few impurities) [44].

327 **3.2. Mass balance of the devolatilization products**

328 A mass balance of coal and biomass samples was conducted by determining the percentage of
329 remaining char after heat treatment and quantifying the mass of light gases including H_2O from
330 devolatilization. Figure 7 shows that there is a deficit beyond the measured char yield and light
331 gases, which indicates that a certain amount of the material is lost in the form of condensable
332 tar and soot during the process. As it can be seen in Figure 7, the variation in the yield of these
333 gas species is greatly affected by changes in the experimental temperature and the
334 carbonaceous materials as well. All parts of the DTF were visually inspected after each
335 devolatilization experiment with no significant amount of heavy volatiles (condensable tars)
336 found on the surfaces of the equipment after CC devolatilization, which could be attributed to
337 the pre-treatment of the starting materials. In contrast, by using visual observation through the
338 viewport on the top water cooled flange it was noticed, that straight after the injection of CC
339 during the experiments, a large amount of soot and fine particle flew out of the crucible with

340 the carrier gas and some particles were found to be trapped in the gas line filter. This behaviour
341 for CC samples could indicate that char fragmentation had occurred during devolatilization at
342 high temperature and caused the deficit in char collection after the rapid heating. It has been
343 reported by other researchers that high heating rate may result in a softening, melting, shrinking
344 and fragmentation in some carbonaceous materials depending on their thermoplasticity [27],
345 [31], [45]. Therefore, it has been speculated that CC has a low thermoplasticity, which resulted
346 in comparatively more fragmentation behaviour in its particles. Previous studies have shown
347 that the presence of low amounts of oily tar gives further evidence of low thermoplasticity for
348 CC as these two properties are strongly linked [46]. As shown in Figure 7, the deficit in the CC
349 increased with increasing the temperature, which confirms that at higher temperature
350 treatments particles are experiencing more extreme heating rate and results in more dust and
351 fine particles formed due to an acceleration in fragmentation.

352 The behaviour of the TC was observed in contrast where large amounts of tar was detected in
353 the filter and on the surfaces of the equipment used. The increase in the heating rate and
354 temperature was found to increase the tar formation, from the result of decrease in the tar
355 condensation at high temperature. Tar condensation reactions are believed to be the dominant
356 phenomena during slow heating/char making (specifically coal coking process), the
357 recombination between solid particles and tar under slow heating leads to form more char and
358 less tar, however during rapid heating the residence time is minimal, causing minimal
359 condensation occurrence and an increase in tar yield [47][48]. Although the temperature
360 increase from 1000 to 1250 °C resulted in an increase in the deficit for thermal coal, at the
361 temperature 1500 °C there was a decrease in the deficit. This behaviour indicates that tar
362 cracking started to occur, which also resulted in an increase in light gases detected by QMS.
363 Furthermore, it can be noted from reagent ultimate analysis results that thermal coal contains

considerable amount of nitrogen, but this has not been detected during devolatilization experiments. Previous literature has shown the fate of N_2 during devolatilization to be largely the conversion to HCN and NH_3 [30], [49]. According to Di Nola et al. [30] the formation of N_2 partitioning is strongly temperature dependant, at the low temperature (≤600 °C) a large portion of N_2 is retained in the char and NH_3 is the main nitrogen gas product. However, at higher temperatures less N_2 is retained, which leads to the formation of large amounts of tar–N, with HCN being the main nitrogen containing gas component at temperature >1300 °C.

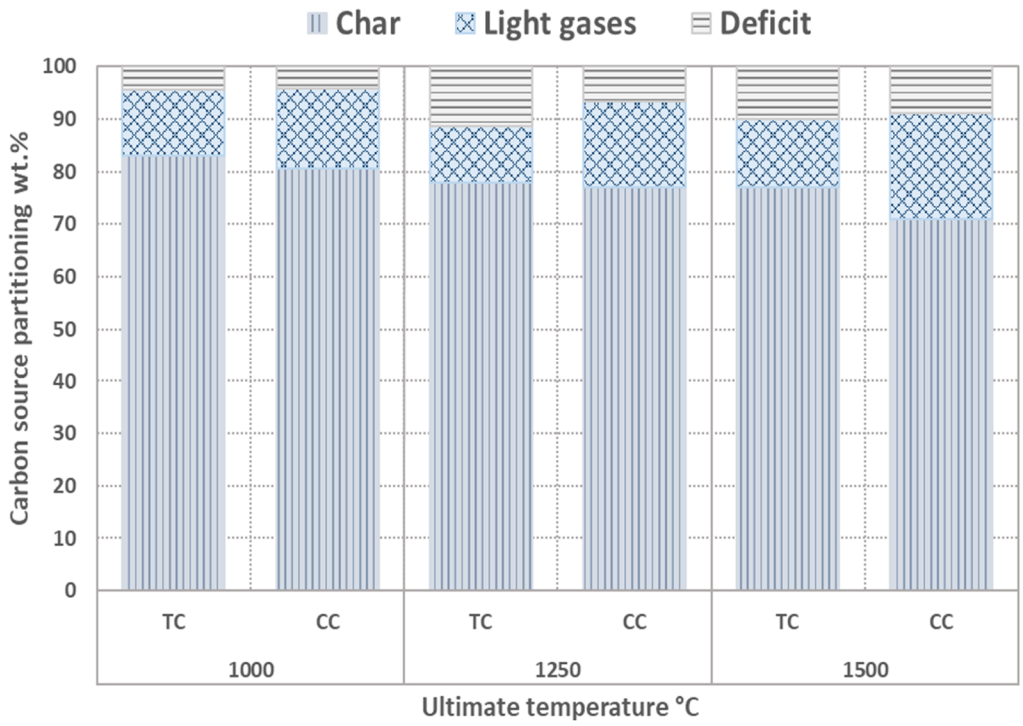

Figure 7. Mass balance of TC and CC during rapid devolatilization experiments at 1000, 1250, and 1500 °C in argon atmosphere.

The weight percentage of gas species formed during rapid devolatilization is presented in Table 2. The results show that gas variations are shifting toward H_2 and CO with an increase in the temperature formed from the thermally enabled secondary reactions. Despite high fixed carbon and low volatile matter content in CC the weight of the residual char collected was lower than

that collected for TC at all temperatures. As mentioned above this could be due to higher particle loss and secondary reactions in CC under rapid heating. As shown in Table 2, both CO_2 and H_2O gas volumes decreased much more significantly for CC with increasing temperature than for TC, which indicates a greater extent of carbon oxidation reaction was completed for CC than TC. This could be due to two phenomena. Firstly CC is more reactive than TC to H_2O and CO_2 due to its more amorphous carbon structure. Secondly as observed a large number of particles had flown with the carrier gas, which resulted in a higher residence time between these particles and light gases formed by devolatilization to enhance the oxidation reactions further.

Table 2 Normalised gas species (wt.%) detected during devolatilization at 1000, 1250 and 1500 °C.

	CO	CO_2	H_2	H_2O	CH_4	C_2H_6
1000 °C						
TC	6.21	15.87	14.36	25.78	29.53	8.26
CC	23.60	31.50	11.21	25.34	7.27	1.09
1250 °C						
TC	35.30	9.23	22.15	20.33	10.79	2.21
CC	61.72	11.14	12.63	10.60	3.28	0.63
1500 °C						
TC	60.78	2.21	20.88	13.96	0.81	1.36
CC	79.11	1.94	13.55	4.29	0.33	0.79

The importance of devolatilization products for pre-reduction in the CCF of HIsarna has been discussed previously, however the iron ore reduction is completed in the SRV by char residuals formed from injected solid carbon through direct/indirect reduction reactions shown in equations (7) to (9). Thus, it is important to know the mount of solid char that will be delivered into the SRV bath after injection of different carbon sources.

$$FeO_{(l)} + Fe\text{–}C_{(l)} \,/\, C_{(s)} \rightarrow Fe_{(l)} + CO_{(g)} \quad (7)$$

$$CO_{(g)} + FeO_{(l)} \rightarrow Fe_{(l)} + CO_{2\,(g)} \quad (8)$$

$$CO_{2\,(g)} + C_{(s)} \rightarrow 2CO_{(g)} \quad (9)$$

By evaluating the R-factor, the ratio of total carbon conversion during rapid devolatilization of carbon materials can be measured to the standard volatile matter (VM) content of the starting materials [28], [35]. The R-factor parameter can give an indication of how efficiently the carbon material can yield solid char residuals under the HIsarna atmosphere. The values of R-factor obtained for the carbonaceous materials used in this investigation are shown in Figure 8.

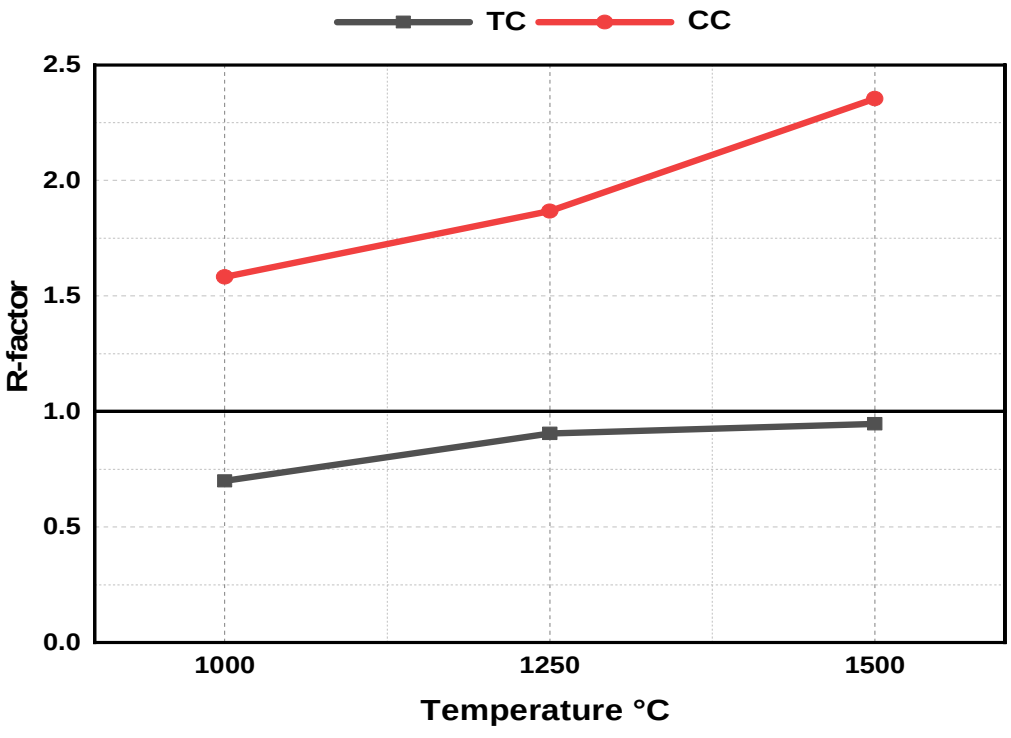

Figure 8. R-factor of TC and CC at reaction temperatures of 1000, 1250, and 1500 °C.

As described by equation 2, a higher R-factor indicates higher conversion of the carbon material during devolatilization. Figure 8 suggests that the value of R-factor increased with an increase in the experimental temperature, therefore the conversion of carbon also increases. The R-factor of TC is smaller than the one of CC at all temperatures which means that TC either fails to completely liberate the volatiles or the recombination of tar and char may take place under these conditions. Despite the low volatile matter content for CC, the R-factor is significantly higher than the one of TC at all temperatures with a maximum value of 2.35 at the peak temperature of 1500 °C. This confirms that large amounts of fixed carbon will be converted into CO during CC injection into HIsarna, which may result in CC being less efficiently delivered to the SRV in comparison to TC. In addition, the extra CO formed during injection of CC may lead to a change in the behaviour of the reactors. Thus it may be advised to enhance the productivity of the CCF to utilise this higher proportion of produced reductive gas to maintain overall efficiency of the process. From the results it should be emphasised that despite the lower VM content in CC, its R-factor is still significantly higher than that for TC. Therefore the devolatilization extent is not determined by VM content only, but it is also controlled by physical and chemical properties of the carbon source.

3.3. Comparison of rapid devolatilisation behaviours for different carbonaceous materials

Several reactions take place simultaneously during rapid heating of the carbonaceous materials, including break-up of chemical bonds, vaporization, and condensation [50]. Previous studies have indicated that the post combustion ratio (PCR) value of reducing gas has an important influence on the pre-reduction degree in the HIsarna's cyclone, which is greatly influenced by carbonaceous materials devolatilization [17], [51]. The total yield of gas products evolved from

the carbon sources (per 1 gram of sample) during rapid heating to the temperatures of 1500 °C is plotted in Figure 9.

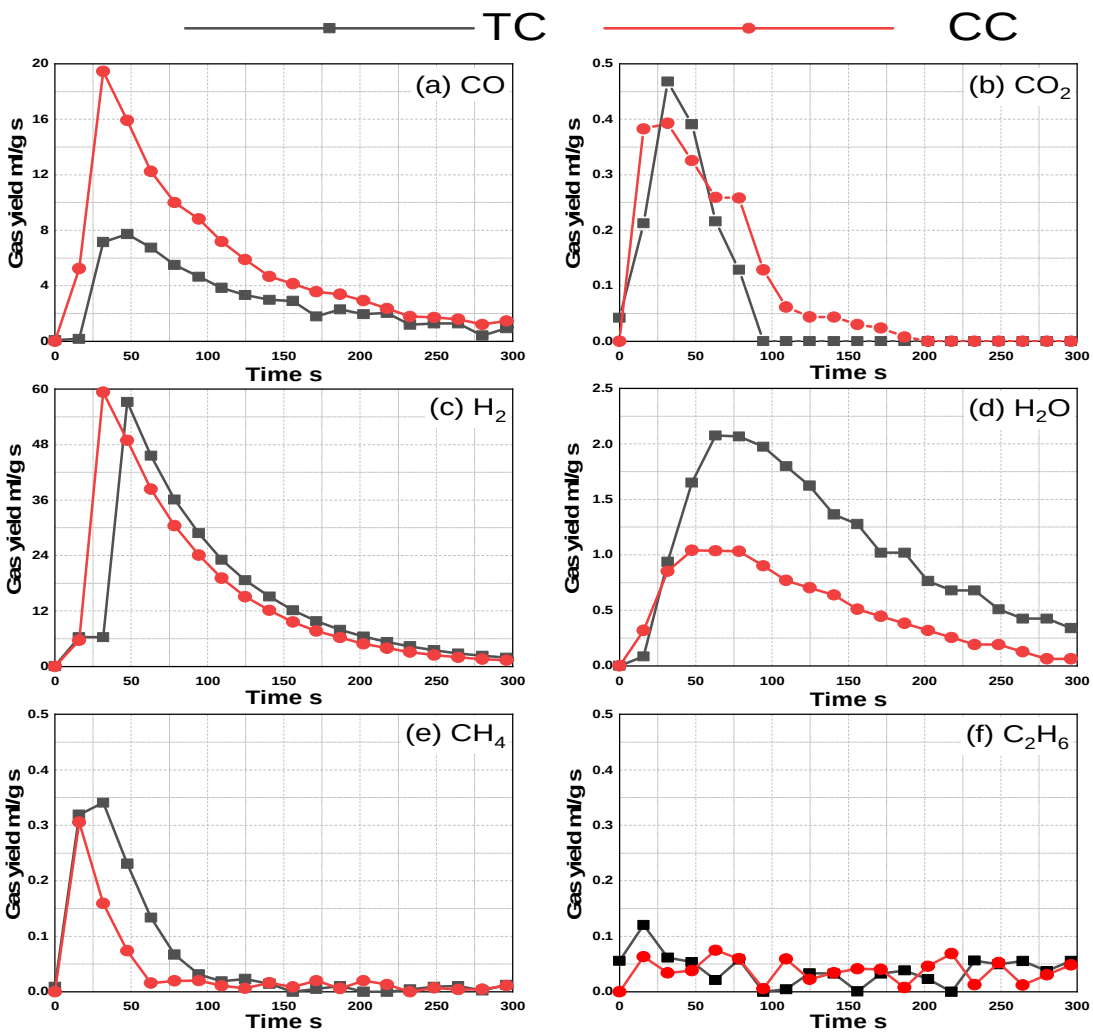

Figure 9. Comparison of gas species yield for (a) CO; (b) CO_2; (c) H_2; (d) H_2O; (e) CH_4; and (f) C_2H_6 produced during rapid devolatilization experiments for TC, and CC under argon atmosphere at 1500 °C.

The evolving of CO_2, H_2O and hydrocarbons are detected earlier than H_2 and CO for both materials. However, CC reaches its peak for both H_2 and CO a few seconds earlier than TC, which may be due to CC having higher reactivity with the surrounding gas atmosphere at temperature of 1500 °C.

436 There are a number of important differences between the materials which will affect the
437 contribution of devolatilization product and the subsequent PCR, and ultimately will affect the
438 pre-reduction within HIsarna. According to equation (1) PCR decreases with an increase of either
439 CO or H_2 or both, and the findings by Chen et al [17] show decrease in the PCR value results in
440 an increase in the pre-reduction degree in the CCF. As shown in Table 3, CC produced
441 significantly larger volumes of CO than TC, however, the difference in H_2 values was minimal.

442 *Table 3. Volume (ml) of gas species detected per gram of sample during 1500 °C devolatilization.*

Materials	CO	CO_2	H_2	H_2O	CH_4	C_2H_6
TC	63.58	1.46	303.67	21.47	1.47	1.41
CC	126.61	1.96	301.43	10.10	0.92	1.25

443 The values in Table 3 indicate that by substituting TC with CC, much lower PCR will be achieved
444 and lead to higher pre-reduction. This is however at the expense of solid carbon char required
445 for SRV productivity/complete reduction. Since about 80% of the reduction takes place in the
446 SRV via gas-slag-metal systems interacting, it is necessary to limit the conversion of carbon
447 materials before they penetrate in the metal bath. CC contains larger amounts of O_2 which is
448 likely to have controlled the variation of gas species and char yield. As mentioned above charcoal
449 conversion is significantly higher than expected due to loss of particles, therefore an increase in
450 the particle size and change in other parameters such as injection rate could help improve the
451 overall efficiency of the low dense CC compared to the use under standard TC process
452 parameters.

453

454 **4. Conclusion**

455 The characteristics and impact of the devolatilization of different carbon sources under high
456 temperature conditions was investigated using DTF-QMS. The effect of change in reaction
457 temperature and the nature of gas species produced during devolatilization process were
458 determined. The following conclusions can be drawn from this study:

459 • There is a significant difference in carbon crystalline structure between TC and CC. The
460 ratio of the intensity of G/D1 in Raman Spectra for CC char is much lower than that for
461 TC char, which indicates that CC has more disordered graphite structure and it is more
462 amorphous carbon, which can lead to higher conversion for CC.
463 • The devolatilization experiments demonstrated the strong impact of temperature on
464 the rate of gas formation, which increases with increasing the temperature. In addition
465 an increase in the temperature results in an increased conversion for both thermal coal
466 and charcoal tested in this study.
467 • The total yield of gaseous species increased with an increase in the devolatilization
468 temperature, and the variation of these gases was greatly affected by an increase in the
469 temperature. The yield of hydrocarbons, CO_2 and H_2O decreases significantly with an
470 increase of temperature, however the yield of both H_2 and CO increase as a
471 consequence. This behaviour indicates that temperature increase can enhance both
472 carbon oxidation and secondary reactions which are taking place during devolatilization.
473 • Similar amounts of H_2 was produced by charcoal and thermal coal at the temperature of
474 1500 ^oC, yet the amount of CO produced by charcoal was twice that of thermal coal. The
475 weight contributed by CO to total gas yield for charcoal at 1000 °C was 23.60%, increased
476 to 61.72% at 1250 °C and subsequently to 79.11% at 1500 °C, this suggests that a large
477 amount of carbon is oxidised by the O_2 functional groups/trapped oxygen within the
478 material itself.

- Despite high fixed carbon and low VM content, charcoal has a high value of R-factor with a maximum value of 2.35 at the temperature of 1500 °C. Due to the fact that conversion degree was much higher than expected with weight loss of 29% at 1500 °C. In contrast the maximum R-factor value for thermal coal is 0.94 at 1500 °C.
- Despite low conversion degree for thermal coal, higher deficits of cumulative material compared to starting mass is observed under all temperatures. It was evidenced that large amounts of heavy volatiles (condensable tar) is formed by thermal coal, and therefore it can be speculated that at the high temperature most of the N_2 components are removed from the char in the form of tar–N and HCN.

Acknowledgement

DK would like to thank Tata Steel Nederland Technology BV for providing the PhD scholarship (Reference No: COL1421/GIPS03241) to carry out this research. ZL would like to appreciate the funding from EPSRC under the grant number EP/N011368/1. The authors appreciate Tata Steel HIsarna team for fruitful discussions and providing samples. DK gratefully acknowledge the kind support by Dr. Ben Breeze at EPR & Diamond Group, University of Warwick for carrying out Raman spectroscopy tests.

References

[1] Z. W. Hu, J. L. Zhang, H. Bin Zuo, M. Tian, Z. J. Liu, and T. J. Yang, "Substitution of biomass for coal and coke in ironmaking process," *Adv. Mater. Res.*, vol. 236–238, pp. 77–82, 2011, doi: 10.4028/www.scientific.net/AMR.236-238.77.

[2] H. Suopajärvi, K. Umeki, E. Mousa, A. Hedayati, H. Romar, A. Kemppainen, C. Wang, A. Phounglamcheik, S. Tuomikoski, N. Norberg, A. Andefors, M. Öhman, U. Lassi, and T.

Fabritius, “Use of biomass in integrated steelmaking – Status quo, future needs and comparison to other low-CO2steel production technologies,” *Appl. Energy*, vol. 213, no. January, pp. 384–407, 2018, doi: 10.1016/j.apenergy.2018.01.060.

[3] S. Jahanshahi, J. G. Mathieson, M. A. Somerville, N. Haque, T. E. Norgate, A. Deev, Y. Pan, D. Xie, P. Ridgeway, and P. Zulli, “Development of Low-Emission Integrated Steelmaking Process,” *J. Sustain. Metall.*, vol. 1, no. 1, pp. 94–114, 2015, doi: 10.1007/s40831-015-0008-6.

[4] F. N. H. Schrama, E. M. Beunder, J. W. K. van Boggelen, R. Boom, and Y. Yang, “Desulphurisation of HIsarna hot metal - a comparison study based on plant data,” *Sci. Technol. Ironmak. Steelmak.*, pp. 419–422, 2017.

[5] R. Sripriya, T. Peeters, K. Meijer, C. Zeilstra, and D. Van Der Plas, “Computational fluid dynamics and combustion modelling of HIsarna incinerator,” *Ironmak. Steelmak.*, vol. 43, no. 3, pp. 192–202, 2016, doi: 10.1179/1743281215Y.0000000031.

[6] J. W. K. Van Boggelen, H. K. A. Meijer, C. Zeilstra, H. Hage, and P. Broersen, “HIsarna - Demonstrating low CO 2 ironmaking at pilot scale,” no. September 2018, pp. 25–27, 1951.

[7] M. Abdul Quader, S. Ahmed, S. Z. Dawal, and Y. Nukman, “Present needs, recent progress and future trends of energy-efficient Ultra-Low Carbon Dioxide (CO2) Steelmaking (ULCOS) program,” *Renew. Sustain. Energy Rev.*, vol. 55, pp. 537–549, 2016, doi: 10.1016/j.rser.2015.10.101.

[8] I. J. Van Der Stel and K. Meijer, “Update to the Developments of Hisarna An Ulcos alternative ironmaking process,” no. November, 2013.

[9] Y. Qu, Y. Yang, Z. Zou, C. Zeilstra, K. Meijer, and R. Boom, “Thermal decomposition

525 behaviour of fine iron ore particles," *ISIJ Int.*, vol. 54, no. 10, pp. 2196–2205, 2014, doi:
526 10.2355/isijinternational.54.2196.

527 [10] Y. Qu, Y. Yang, Z. Zou, C. Zeilstra, K. Meijer, and R. Boom, "Kinetic study on gas molten
528 particle reduction of iron ore fines at high temperature," *Ironmak. Steelmak.*, vol. 42,
529 no. 10, pp. 763–773, 2015, doi: 10.1179/1743281215Y.0000000021.

530 [11] K. Meijer, C. Guenther, and R. J. Dry, "HIsarna Pilot Plant Project," *InSteelCon*, no. July,
531 pp. 1–5, 2011.

532 [12] Y. Cheng, B. H. Yan, C. X. Cao, Y. Cheng, and Y. Jin, "Experimental investigation on coal
533 devolatilization at high temperatures with different heating rates," *Fuel*, vol. 117, no.
534 PARTB, pp. 1215–1222, 2014, doi: 10.1016/j.fuel.2013.08.016.

535 [13] E. Biagini, M. Simone, and L. Tognotti, "Characterization of high heating rate chars of
536 biomass fuels," *Proc. Combust. Inst.*, vol. 32 II, no. 2, pp. 2043–2050, 2009, doi:
537 10.1016/j.proci.2008.06.076.

538 [14] L. Chen, C. Zeng, X. Guo, Y. Mao, Y. Zhang, X. Zhang, W. Li, Y. Long, H. Zhu, B. Eiteneer,
539 and V. Zamansky, "Gas evolution kinetics of two coal samples during rapid pyrolysis,"
540 *Fuel Process. Technol.*, vol. 91, no. 8, pp. 848–852, 2010, doi:
541 10.1016/j.fuproc.2010.02.010.

542 [15] Y. Qu, Y. Yang, Z. Zou, C. Zeilstra, K. Meijer, and R. Boom, "Reduction kinetics of fine
543 hematite ore particles with a high temperature drop tube furnace," *ISIJ Int.*, vol. 55, no.
544 5, pp. 952–960, 2015, doi: 10.2355/isijinternational.55.952.

545 [16] Y. Qu, *Experimental Study of the Melting and Reduction Behaviour of Ore Used in the*
546 *HIsarna Process PhD thesis Yingxia Qu*. 2013.

547 [17] Z. Chen, Y. Qu, C. Zeilstra, J. van der Stel, J. Sietsma, and Y. Yang, "Thermodynamic

548 evaluation for reduction of iron oxide ore particles in a high temperature drop tube
549 furnace," *Ironmak. Steelmak.*, vol. 47, no. 2, pp. 173–177, 2020, doi:
550 10.1080/03019233.2018.1498762.

551 [18] Y. Qu, Y. Yang, Z. Zou, C. Zeilstra, K. Meijer, and R. Boom, "Melting and reduction
552 behaviour of individual fine hematite ore particles," *ISIJ Int.*, vol. 55, no. 1, pp. 149–157,
553 2015, doi: 10.2355/isijinternational.55.149.

554 [19] A. A. El-Tawil, L. S. Ökvist, H. M. Ahmed, and B. Björkman, "Devolatilization kinetics of
555 different types of bio-coals using thermogravimetric analysis," *Metals (Basel).*, vol. 9,
556 no. 2, pp. 1–13, 2019, doi: 10.3390/met9020168.

557 [20] Y. Qiao, S. Chen, Y. Liu, H. Sun, S. Jia, J. Shi, C. M. Pedersen, Y. Wang, and X. Hou,
558 "Pyrolysis of chitin biomass: TG-MS analysis and solid char residue characterization,"
559 *Carbohydr. Polym.*, vol. 133, pp. 163–170, 2015, doi: 10.1016/j.carbpol.2015.07.005.

560 [21] X. Li, G. Matuschek, M. Herrera, H. Wang, and A. Kettrup, "Investigation of pyrolysis of
561 Chinese coals using thermal analysis/mass spectrometry," *J. Therm. Anal. Calorim.*, vol.
562 71, no. 2, pp. 601–612, 2003, doi: 10.1016/s0140-6701(04)90448-1.

563 [22] A. Arenillas, F. Rubiera, and J. J. Pis, "Simultaneous thermogravimetric-mass
564 spectrometric study on the pyrolysis behaviour of different rank coals," *J. Anal. Appl.*
565 *Pyrolysis*, vol. 50, no. 1, pp. 31–46, 1999, doi: 10.1016/S0165-2370(99)00024-8.

566 [23] F. Han, A. Meng, Q. Li, and Y. Zhang, "Thermal decomposition and evolved gas analysis
567 (TG-MS) of lignite coals from Southwest China," *J. Energy Inst.*, vol. 89, no. 1, pp. 94–
568 100, 2016, doi: 10.1016/j.joei.2015.01.007.

569 [24] K. Jayaraman, M. V. Kok, and I. Gokalp, "Thermogravimetric and mass spectrometric
570 (TG-MS) analysis and kinetics of coal-biomass blends," *Renew. Energy*, vol. 101, pp.

293–300, 2017, doi: 10.1016/j.renene.2016.08.072.

[25] K. Zhang, Z. Wang, W. Fang, Y. He, E. Hsu, Q. Li, J. Gul-e-Rana, and K. Cen, “High-temperature pyrolysis behavior of a bituminous coal in a drop tube furnace and further characterization of the resultant char,” *J. Anal. Appl. Pyrolysis*, vol. 137, no. August 2018, pp. 163–170, 2019, doi: 10.1016/j.jaap.2018.11.022.

[26] S. B. Liaw and H. Wu, “A New Method for Direct Determination of Char Yield during Solid Fuel Pyrolysis in Drop-Tube Furnace at High Temperature and Its Comparison with Ash Tracer Method,” *Energy and Fuels*, vol. 33, no. 2, pp. 1509–1517, 2019, doi: 10.1021/acs.energyfuels.8b03161.

[27] J. Yu, J. A. Lucas, and T. F. Wall, “Formation of the structure of chars during devolatilization of pulverized coal and its thermoproperties: A review,” *Prog. Energy Combust. Sci.*, vol. 33, no. 2, pp. 135–170, 2007, doi: 10.1016/j.pecs.2006.07.003.

[28] W. H. Chen, S. W. Du, and T. H. Yang, “Volatile release and particle formation characteristics of injected pulverized coal in blast furnaces,” *Energy Convers. Manag.*, vol. 48, no. 7, pp. 2025–2033, 2007, doi: 10.1016/j.enconman.2007.01.001.

[29] J. Tanner and S. Bhattacharya, “Kinetics of CO2 and steam gasification of Victorian brown coal chars,” *Chem. Eng. J.*, vol. 285, pp. 331–340, 2016, doi: 10.1016/j.cej.2015.09.106.

[30] G. Di Nola, W. de Jong, and H. Spliethoff, “The fate of main gaseous and nitrogen species during fast heating rate devolatilization of coal and secondary fuels using a heated wire mesh reactor,” *Fuel Process. Technol.*, vol. 90, no. 3, pp. 388–395, 2009, doi: 10.1016/j.fuproc.2008.10.009.

[31] E. Biagini, P. Narducci, and L. Tognotti, “Size and structural characterization of lignin-

cellulosic fuels after the rapid devolatilization," *Fuel*, vol. 87, no. 2, pp. 177–186, 2008, doi: 10.1016/j.fuel.2007.04.010.

[32] J. Li, G. Bonvicini, L. Tognotti, W. Yang, and W. Blasiak, "High-temperature rapid devolatilization of biomasses with varying degrees of torrefaction," *Fuel*, vol. 122, pp. 261–269, 2014, doi: 10.1016/j.fuel.2014.01.012.

[33] S. F. Zhang, F. Zhu, G. Bai, L. Y. Wen, and H. J. Peng, "High temperature pyrolysis behaviour and kinetics of lump coal in COREX melter gasifier," *Ironmak. Steelmak.*, vol. 41, no. 3, pp. 219–228, 2014, doi: 10.1179/1743281213Y.0000000122.

[34] W. H. Chen and J. S. Wu, "An evaluation on rice husks and pulverized coal blends using a drop tube furnace and a thermogravimetric analyzer for application to a blast furnace," *Energy*, vol. 34, no. 10, pp. 1458–1466, 2009, doi: 10.1016/j.energy.2009.06.033.

[35] W. H. Chen, S. W. Du, C. H. Tsai, and Z. Y. Wang, "Torrefied biomasses in a drop tube furnace to evaluate their utility in blast furnaces," *Bioresour. Technol.*, vol. 111, pp. 433–438, 2012, doi: 10.1016/j.biortech.2012.01.163.

[36] G. Wang, J. Zhang, G. Zhang, X. Ning, X. Li, Z. Liu, and J. Guo, "Experimental and kinetic studies on co-gasification of petroleum coke and biomass char blends," *Energy*, vol. 131, pp. 27–40, 2017, doi: 10.1016/j.energy.2017.05.023.

[37] X. A. Huang, K. W. Ng, L. Giroux, and M. Duchesne, "Carbonaceous Material Properties and Their Interactions with Slag During Electric Arc Furnace Steelmaking," *Metall. Mater. Trans. B Process Metall. Mater. Process. Sci.*, vol. 50, no. 3, pp. 1387–1398, 2019, doi: 10.1007/s11663-019-01569-1.

[38] D. Khasraw, S. Spooner, H. Hage, K. Meijer, and Z. Li, "Devolatilisation characteristics of coal and biomass with respect to temperature and heating rate for HIsarna alternative

ironmaking process," *Fuel*, vol. 284, no. July 2020, p. 119101, 2021, doi: 10.1016/j.fuel.2020.119101.

[39] V. Krishnamoorthy, Y. D. Yeboah, and S. V. Pisupati, "Influence of pyrolysis gas on volatile yield and co 2 reaction kinetics of the char samples generated in a high-pressure, high-temperature flow reactor," *Energies*, vol. 12, no. 1, 2019, doi: 10.3390/en12010107.

[40] X. Huang, D. Kocaefe, and Y. Kocaefe, "Utilization of Biocoke as a Raw Material for Carbon Anode Production," *Energy and Fuels*, vol. 32, no. 8, pp. 8537–8544, 2018, doi: 10.1021/acs.energyfuels.8b01832.

[41] G. Wang, J. Zhang, X. Hou, J. Shao, and W. Geng, "Study on CO2 gasification properties and kinetics of biomass chars and anthracite char," *Bioresour. Technol.*, vol. 177, pp. 66–73, 2015, doi: 10.1016/j.biortech.2014.11.063.

[42] A. Basile, G. Centi, M. De Falco, and G. Iaquaniello, "The vision of future sustainable energy, catalyst, and chemistry: Opportunities for innovation and business," *Studies in Surface Science and Catalysis*. 2019, doi: 10.1016/B978-0-444-64337-7.00001-X.

[43] M. M. Halmann, *Chemical Fixation of Carbon DioxideMethods for Recycling CO2 into Useful Products*. 2018.

[44] A. Abánades, C. Rubbia, and D. Salmieri, "Thermal cracking of methane into Hydrogen for a CO2-free utilization of natural gas," *Int. J. Hydrogen Energy*, vol. 38, no. 20, pp. 8491–8496, 2013, doi: 10.1016/j.ijhydene.2012.08.138.

[45] I. A. Moore, "Direct Observation of Swelling Coal Particles," no. October, 2018.

[46] M. Fraga, B. Flores, E. Osório, and A. Vilela, "Evaluation of the thermoplastic behavior of charcoal, coal tar and coking coal blends," *J. Mater. Res. Technol.*, vol. 9, no. 3, pp.

3406–3410, 2020, doi: 10.1016/j.jmrt.2020.01.076.

[47] J. Wu, Q. Liu, R. Wang, W. He, L. Shi, X. Guo, Z. Chen, L. Ji, and Z. Liu, “Coke formation during thermal reaction of tar from pyrolysis of a subbituminous coal,” *Fuel Process. Technol.*, 2017, doi: 10.1016/j.fuproc.2016.03.022.

[48] K. H. van Heek and W. Hodek, “Structure and pyrolysis behaviour of different coals and relevant model substances,” *Fuel*, vol. 73, no. 6, pp. 886–896, 1994, doi: 10.1016/0016-2361(94)90283-6.

[49] J. Leppälahti and T. Koljonen, “Nitrogen evolution from coal, peat and wood during gasification: Literature review,” *Fuel Process. Technol.*, vol. 43, no. 1, pp. 1–45, 1995, doi: 10.1016/0378-3820(94)00123-B.

[50] R. Xu, J. Zhang, G. Wang, H. Zuo, Z. Liu, K. Jiao, Y. Liu, and K. Li, “Devolatilization Characteristics and Kinetic Analysis of Lump Coal from China COREX3000 Under High Temperature,” *Metall. Mater. Trans. B Process Metall. Mater. Process. Sci.*, vol. 47, no. 4, pp. 2535–2548, 2016, doi: 10.1007/s11663-016-0708-8.

[51] Z. Chen, C. Zeilstra, J. van der Stel, J. Sietsma, and Y. Yang, “Review and data evaluation for high-temperature reduction of iron oxide particles in suspension,” *Ironmak. Steelmak.*, vol. 0, no. 0, pp. 1–7, 2019, doi: 10.1080/03019233.2019.1589755.